ISA Transactions 135 (2023) 1–12

Contents lists available at ScienceDirect

ISA Transactions

journal homepage: www.elsevier.com/locate/isatrans

Research article

Event-triggered interval estimation method for cyber–physical systems with unknown inputs

Jun Huang [a,*], Jianwei Fan [a], Thach Ngoc Dinh [b], Xudong Zhao [c], Yueyuan Zhang [a]

[a] The School of Mechanical and Electrical Engineering, Soochow University, Suzhou 215131, China
[b] Conservatoire National des Arts et Métiers (CNAM), Cedric-Lab, 292, Rue Saint-Martin 75141 Paris Cedex 03, France
[c] The School of Control Science and Engineering, Dalian University of Technology, Dalian 116000, China

ARTICLE INFO

Article history:
Received 10 May 2022
Received in revised form 4 September 2022
Accepted 10 September 2022
Available online 20 September 2022

Keywords:
Cyber–physical systems
Event-triggered observer
Unknown inputs
Descriptor systems

ABSTRACT

The issue of secure estimation for cyber–physical systems subject to unknown inputs and stealthy deception attacks is addressed in this paper. First, the unknown inputs are treated as augmented state and on the basis of that, the original plant is transformed into a singular system, which is decoupled with the unknown inputs. Then, for the purpose of reducing communication burden and avoiding congestion in the network, the event-triggered mechanism is introduced. Two approaches are presented to accomplish state estimation. The former one is known as the monotone system method. In the latter method, an input-to-state stable robust observer is constructed and by using the set-membership method, approximated estimation error is obtained. Finally, the effectiveness of the proposed method is verified by two illustrative examples.

1. Introduction

Recently, The issue of state estimation (SE) for cyber–physical systems (CPSs) has attracted considerable attention in the field of control theory. For the physical part of CPSs, there are multiple challenges faced by the researchers. To begin with, how to accomplish SE for various complex systems, such as switched systems [1], time-varying systems [2], stochastic systems [3], etc., is a laborious problem. Additionally, external factors such as disturbances and unknown inputs (UIs), make SE a tougher problem to solve. Generally speaking, UIs are difficult to deal with since there is no prior knowledge about them. Gang et al. [4] constructed an UI observer which involves only the past and actual values of the system output. However, it is worth noting that the observer matching condition is required to be satisfied, which is a noticeable constraint. In this paper, the UIs are treated as an augmented state and on the basis of that, the original system is equivalently transformed into a singular system.

Compared with UIs, disturbances are a kind of factors that imposed on the system more frequently. The assumption that the disturbances are unknown but bounded is commonly made by the researchers, since it conforms to reality. To solve the SE problem for systems with bounded disturbances, the interval observers (IOs) are usually considered as an effective tool. With the information of inputs and outputs and bounded disturbances, the IOs are able to guarantee the nonnegativity of error dynamics. Moreover, by designing an appropriate observer gain, real-time tracking of the states can be realized by upper and lower bounds of the interval. Thus, the design of IOs has drawn numerous concerns [5–8]. Generally speaking, the application of IOs in control theory is mainly reflected in two aspects. One is for the state reconstruction. Up to now, IO design problem for a series of complicated systems has been addressed which includes nonlinear time-varying systems [2], LPV systems [9], switched linear systems [10] and so on. On the other hand, the IOs are also used for feedback control or coordinate control. For instance, Wang Y. et al. [11] constructed IOs for linear switched systems and on the basis of that, event-triggered control scheme was designed where the states of the IOs are utilized for feedback. Similarly, Wang X. et al. [12] constructed distributed IOs for networked systems and then designed an IO-based control protocol which is able to drive the plant to realize coordinate behavior.

For the cyber part of CPSs, challenges exist as well. First of all, security issues are significant since they have a direct bearing on property and human security. Nowadays, under the threat of various types of cyber attacks, including denial-of-service attacks, replay attacks, and deception attacks, corresponding countermeasures need to be elaborated. Thus, attack detection [13], attack recovery [14], resilient control [15] and other issues have become a hot topic. In addition, with the accelerated popularization of the Internet and the blowout growth of global network demand and web traffic, how to improve the utilization of network resources is another challenge faced by CPSs. To solve

* Corresponding author.
E-mail addresses: cauchyhot@163.com (J. Huang), 15058428720@163.com (J. Fan), ngoc-thach.dinh@lecnam.net (T.N. Dinh), xudongzhao@dlut.edu.cn (X. Zhao), yueyuanzhang@126.com (Y. Zhang).

https://doi.org/10.1016/j.isatra.2022.09.020
0019-0578/

this problem, the event-triggered mechanism (ETM) has been proposed and received more and more attention in recent years [16–18]. Compared with the traditional sampled-data schemes, data transmission under event-triggered protocol only occurs when a specific event is triggered, usually when a presupposed condition is violated. However, it should be realized that the employment of ETM is often accompanied by the deterioration of system performance due to the hysteresis of information. Moreover, an inherent problem naturally brought by the ETM is the possibilities of Zeno behavior [19], i.e., infinite triggering in finite time.

Concerning SE problem of CPSs under cyber attacks, especially stealthy deception attacks, there are a few researches reported in the literature such as [8,20]. Huong et al. [8] addressed the problem of functional IO design for time-delay systems under stealthy attacks while Li et al. [20] designed IOs for a class of CPSs using an improved event-triggered protocol. It is worth pointing out that, [5,6] put their attention on conventional IO design for systems without security risk; and [8,20] addressed the SE problem for CPSs under cyber attacks. However, as mentioned above, the introduction of UIs will remarkably increase the difficulty of the SE problem. Predictably, SE under the co-existence of cyber attacks and UIs remains a challenging work. Moreover, to the best of the authors' knowledge, the research of event-triggered IO (ETIO) design for CPSs subject to UIs and stealthy attacks has rarely been reported.

Motivated by the above discussion, this paper focuses on event-triggered secure estimation for CPSs subject to UIs. The contribution of this paper lies in four parts: (i) ETIOs for cyber–physical systems are considered in this paper, while most existing work focused on IO design for conventional systems; (ii) The co-existence of stealthy attacks and UIs are contained in CPSs, which makes the design much more challenging. (iii) The UIs are treated as augmented states and decoupled from the descriptor system. Reachable set analysis is employed to reduce the effect caused by the stealthy attacks. (iv) The H_∞ set-membership technique is used to relax the constraints of the traditional methods, and it is characterized by higher accuracy in interval estimation. The structure of this article is outlined as follows: The problem is formulated and preliminaries are presented in Section 2; The main results of this paper is given in Section 3; Section 4 provides illustrative examples to verify the effectiveness of the proposed method.

Notations

In this paper, $\rangle$, $\langle$ should be understood elementwise for vectors. For matrices A and B, $A \succ (\prec)\ B$ means that $A - B$ is positive (negative) definite. The symbols R^a and $R^{a\times b}$ denote the Euclidean space with dimension a and $a \times b$, respectively. For a matrix S, $S^+ = \max\{0,\ S\}$, $S^- = S^+ - S$. The matrix I denotes identity matrix with appropriate dimensions. The symbols $\oplus$ and $\odot$ stand for the Minkowski sum and the linear mapping, respectively.

2. Preliminaries and problem formulation

Consider a CPS with UIs, which is modeled by

$$\begin{cases} x(k+1) = Ax(k) + Bu(k) + J\omega(k) + Dd(k), \\ y(k) = Cx(k) + Fd(k), \end{cases} \tag{1}$$

where $x(k) \in R^{n_x}$, $u(k) \in R^{n_u}$, $\omega(k) \in R^{n_\omega}$, $d(k) \in R^{n_d}$, $y(k) \in R^{n_y}$ are the state, the control input, the disturbance, the UI and the measured output, respectively. $A \in R^{n_x\times n_x}$, $B \in R^{n_x\times n_u}$, $C \in R^{n_y\times n_x}$, $D \in R^{n_x\times n_d}$, $F \in R^{n_y\times n_d}$, $J \in R^{n_x\times n_\omega}$ are known constant matrices. To alleviate the network congestion, an event-triggered protocol is introduced in this paper. Denote $y^t(k)$ as the event-triggered measurement output received by the observer at the time instant k. The trigger condition is formulated as

$$e_y^T(k)e_y(k) < \delta y^T(k)y(k), \tag{2}$$

where $e_y(k) = y^t(k) - y(k)$ and δ is the triggering threshold adjusting the triggering frequency. The ETM intends to send $y(k)$ to the observer when (2) is violated.

Assumption 2.1. The following inequalities hold for the initial state $x(0)$ and the disturbance $\omega(k)$ of system (1)

$$\underline{x} \le x(0) - p_0 \le \bar{x}, \quad \underline{\omega} \le \omega(k) \le \bar{\omega} \tag{3}$$

where $\underline{x} = -\bar{x}$, $\underline{\omega} = -\bar{\omega}$. $p_0 \in R^{n_x}$, $\bar{x} \in R^{n_x}$, and $\bar{\omega} \in R^{n_\omega}$ are all known vectors.

Moreover, the cyber attacks in the transmission of signal $y^t(k)$ is taken into account. It is assumed that the adversaries have access to the matrices A, B, C and J, however, due to limited resources and knowledge, they are not aware of the fact that the system is affected by UIs, i.e., the attackers consider the model of system as

$$\begin{cases} x(k+1) = Ax(k) + Bu(k) + J\omega(k), \\ y(k) = Cx(k). \end{cases} \tag{4}$$

The adversaries intend to disrupt the information sent to the observer by injecting bias $b(k)$ to $y^t(k)$ such that the information received by the observer is $y_b^t(k) = y^t(k) + b(k)$. In addition, to avoid being detected, the adversaries formulate their attack strategies as follows.

Definition 2.1 (*[21]*)**.** Given a nonzero vector $b(k)$, if the following equation

$$y_b(x^I(0), \omega^I(k-1), b(k)) = y(x^{II}(0), \omega^{II}(k-1)) \tag{5}$$

holds for two distinct initial conditions $x^I(0), x^{II}(0) \in [p_0 + \underline{x}, p_0 + \bar{x}]$, then $b(k)$ is called a stealthy attack against system (4). $y_b(x^I(0), \omega^I(k-1), b(k)) = y(x^I(0), \omega^I(k-1)) + b(k)$ denotes the expected compromised output from the attackers' perspective. $y(x^{II}(0), \omega^{II}(k-1))$ denotes the measured output driven by distinct initial conditions under zero attack.

Remark 2.1. It is noteworthy that the aforementioned hypothesis that the attackers have access to limited information and resources is widely seen in the literature [22–24]. The adversaries formulate attack policy according to limited information, however, since the plant is affected by the UIs and the ETM is considered during data transmission, the eventual effect of the injected bias may be different from what is expected by the adversaries.

Remark 2.2. This paper aims to achieving interval estimation of state vector $x(k)$ for plant (1) subject to UIs and stealthy attacks via two methods. The first one is known as the monotone system (MS) method and the second one is the set-membership (SM) method. For the convenience of understanding, the above discussion can be summarized as Fig. 1.

Some definitions and properties about the SM theory are reviewed in what follows.

Definition 2.2. For vectors $v_i, i = 1, \ldots, n$, if there exist vectors p_i and q_i such that $p_i \le v_i \le q_i$, then

$$\boldsymbol{v} = \{v : v \in R^n, p_i \le v_i \le q_i, i = 1, \ldots, n\}, \tag{6}$$

is called an interval vector. Moreover, $\boldsymbol{v}$ can be reformulated as

$$\boldsymbol{v} = [p, q], \tag{7}$$

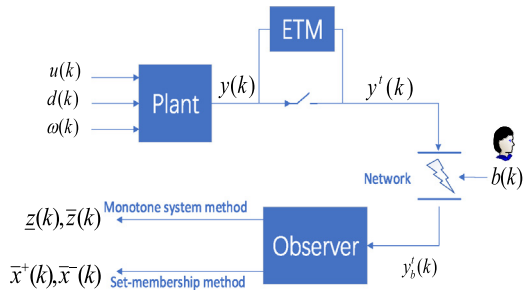

Fig. 1. The structure of this paper.

where $p = [p_1, \ldots, p_n]^T$ and $q = [q_1, \ldots, q_n]^T$. Furthermore, an interval vector $\boldsymbol{v} \subset R^m$ is called a hypercube $\boldsymbol{H}^m$, if all its elements are equivalent to $[-1, 1]$.

Definition 2.3. The interval hull of a given set $\boldsymbol{\Omega} \in R^n$ is defined as the smallest interval vector that contains it, which can be expressed by

$$\boldsymbol{\Omega} \subseteq \mathcal{H}(\boldsymbol{\Omega}) = [p, q]. \tag{8}$$

Property 2.1. *Concerning a series of sets $\boldsymbol{\Omega_i} \subset R^n, i = 1, \ldots, m$, it holds that*

$$\mathcal{H}(\bigoplus_{i=1}^{m} \boldsymbol{\Omega_i}) = \bigoplus_{i=1}^{m} \mathcal{H}(\boldsymbol{\Omega_i}). \tag{9}$$

where $\bigoplus$ denotes the Minkowski sum of a series of sets.

Definition 2.4. The affine transformation of a k-order hypercube $\boldsymbol{H}^k$, i.e.,

$$\boldsymbol{\Pi} \triangleq \langle p, Q \rangle = \langle p + Qx, x \in \boldsymbol{H}^k \rangle, \tag{10}$$

is called a zonotope, whose center is $p \in R^n$ and its shape and volume are determined by the generator matrix $Q \in R^{n \times m}$.

Property 2.2. *The following equalities hold for zonotopes:*

$$\begin{aligned} \langle p_1, Q_1 \rangle \oplus \langle p_2, Q_2 \rangle &= \langle p_1 + p_2, [Q_1, Q_2] \rangle, \\ F \odot \langle p, Q \rangle &= \langle Fp, FQ \rangle, \\ \langle p, Q \rangle &\in \langle p, \bar{Q} \rangle, \end{aligned} \tag{11}$$

where $p_1, p_2, p \in R^n, Q_1, Q_2, Q \in R^{a \times b}$, and $F \in R^{l \times b}$. $\bar{Q}$ is a diagonal matrix whose diagonal elements are determined by

$$\bar{Q}_{i,i} = \sum_{j=1}^{b} |Q_{i,j}|, i = 1, \ldots, a. \tag{12}$$

Property 2.3. *Given a zonotope $\boldsymbol{\Pi} = \langle p, Q \rangle \subset R^a$, $Q \in R^{a \times b}$, the components of its interval hull $\mathcal{H}(\boldsymbol{\Pi}) = [x, y]$ are determined by*

$$\begin{cases} x_i = p_i - \sum_{j=0}^{b} |Q_{i,j}|, i = 1, \ldots, a, \\ y_i = p_i + \sum_{j=0}^{b} |Q_{i,j}|, i = 1, \ldots, a. \end{cases} \tag{13}$$

On account of Definition 2.4, one can rewrite (3) as:

$$x(0) \in \langle p_0, Q_0 \rangle, \quad \omega(k) \in \langle 0, D_\omega \rangle \triangleq \mathbf{W}, \tag{14}$$

where Q_0, D_ω are diagonal matrices whose diagonal elements are equivalent to the corresponding elements in $x(0), \omega(k)$.

Lemma 2.1. *If Assumption 2.1 holds, then the injected bias $b(k)$ is a bounded vector against the system (4) with its upper and lower bounds being determined by*

$$\begin{aligned} [\underline{b}(k), \bar{b}(k)] &= \mathcal{H}(\mathcal{B}) \\ &= \mathcal{H}(CA^k \langle 0, 2Q_0 \rangle) \oplus \bigoplus_{i=0}^{k-1} \mathcal{H}(2CA^i B\mathbf{W}), \end{aligned} \tag{15}$$

where $\mathcal{B}$ represents the reachable set of $b(k)$, which is calculated by

$$\mathcal{B} = CA^k \langle 0, 2Q_0 \rangle \oplus \bigoplus_{i=0}^{k-1} 2CA^i B\mathbf{W}. \tag{16}$$

Proof. To begin with, the following equation holds according to Definition 2.1,

$$y(x(0)^I, \omega(k-1)^I) + b(k) = y(x(0)^{II}, \omega(k-1)^{II}), \tag{17}$$

which means

$$b(k) = C\Xi(k), \tag{18}$$

where $\Xi(k) = x(x(0)^{II}, \omega(k-1)^{II}) - x(x(0)^I, \omega(k-1)^I)$. Since $\Xi(0) = (x(0)^{II} - x(0)^I) \in \langle 0, 2Q_0 \rangle$, it can be deduced that

$$\Xi(k+1) = A\Xi(k) + B(\omega(k)^{II} - \omega(k)^I). \tag{19}$$

According to (18) and (19), $b(k)$ can be calculated by

$$\begin{aligned} b(k) =& C\Xi(k) \\ =& C[A\Xi(k-1) + B(\omega(k-1)^{II} - \omega(k-1)^I)] \\ =& \cdots \\ =& CA^k\Xi(0) + C\sum_{i=0}^{k-1} A^i B(\omega(k-1-i)^{II} \\ & - \omega(k-1-i)^I). \end{aligned} \tag{20}$$

Define $\mathcal{B}$ as the reachable set of $b(k)$, it is derived that

$$\mathcal{B} = CA^k \langle 0, 2Q_0 \rangle \oplus \bigoplus_{i=0}^{k-1} 2CA^i B\mathbf{W}. \tag{21}$$

Finally, one can compute the interval hull of $\mathcal{B}$ by

$$\begin{aligned} [\underline{b}(k), \bar{b}(k)] =& \mathcal{H}(\mathcal{B}) \\ =& \mathcal{H}(CA^k \langle 0, 2Q_0 \rangle) \oplus \bigoplus_{i=0}^{k-1} \mathcal{H}(2CA^i B\mathbf{W}). \end{aligned} \tag{22}$$

The proof is completed here.

To simplify ETIO design, the system (1) is supposed to be decoupled from the UI $d(k)$, to this end, we consider it as augmented states, i.e., $\bar{x}(k) = \begin{bmatrix} x^T(k) & d^T(k) \end{bmatrix}^T$, consequently, (1) is transformed into

$$\begin{cases} E\bar{x}(k+1) = \bar{A}\bar{x}(k) + \bar{B}u(k) + \bar{J}\omega(k), \\ y(k) = \bar{C}\bar{x}(k), \end{cases} \tag{23}$$

where

$$\begin{aligned} E &= \begin{bmatrix} I_{n_x} & 0 \\ 0 & 0_{n_d} \end{bmatrix}, \bar{A} = \begin{bmatrix} A & D \\ 0 & 0_{n_d} \end{bmatrix}, \\ \bar{B} &= \begin{bmatrix} B \\ 0 \end{bmatrix}, \bar{J} = \begin{bmatrix} J \\ 0 \end{bmatrix}, \bar{C} = \begin{bmatrix} C & F \end{bmatrix}. \end{aligned} \tag{24}$$

Obviously, we have $rank(E) < n_x + n_d$, thus, the original system (1) is transformed into a descriptor system (23). Without loss of generality, it is assumed that the matrix $\begin{bmatrix} E^T & \bar{C}^T \end{bmatrix}^T$ is of full column rank.

Remark 2.3. When the UIs only appear in the system equation, it is easy to design a reduced-order UI observer. However, it becomes more challenging when the entire system is affected by the UIs. To deal with this problem, UI decoupling and state transformation were employed in [25]. However, the minimal phase condition and the observer matching condition are required to be satisfied, thereby resulting in significant conservatism. In response to this, we combine the UIs with the state vector as an augmented vector. Consequently, the original system suffered from UIs can be equivalently transformed into a singular system which is immune to the UIs. Such an approach imposes no prior conditions and we only need to deal with the descriptor system.

3. Main result

In the section, we provide two approaches to design ETIOs for CPS with UIs.

Lemma 3.1 (*[26]*). *Given a matrix equation $MN = O$, where $M \in R^{p\times q}$, $N \in R^{q\times t}$, $O \in R^{p\times t}$, if $rank(N) = t$, then the general solution of it is*

$$M = ON^{\dagger} + S[I_b - NN^{\dagger}], \tag{25}$$

where $N^{\dagger}$ denotes the pseudo inverse matrix of N, $S \in R^{p\times q}$ is an arbitrary matrix.

For the equation $\Phi E+\Psi \bar{C} = I_{n_x+n_d}$, where $\Phi \in R^{(n_x+n_d)\times(n_x+n_d)}$, $\Psi \in R^{(n_x+n_d)\times n_y}$ are matrices to be determined, since the matrices E and $\bar{C}$ of the descriptor system (23) satisfy

$$rank\left(\begin{bmatrix} E \\ \bar{C} \end{bmatrix}\right) = rank\left(\begin{bmatrix} I_{n_x} & 0 \\ 0 & 0_{n_d} \\ C & F \end{bmatrix}\right) = n_x + n_d. \tag{26}$$

Then according to Lemma 3.1, a possible solution of the equation is

$$\begin{bmatrix} \Phi & \Psi \end{bmatrix} = \begin{bmatrix} E \\ \bar{C} \end{bmatrix}^{\dagger} + S(I_{n_d+n_x+n_y} - \begin{bmatrix} E \\ \bar{C} \end{bmatrix}\begin{bmatrix} E \\ \bar{C} \end{bmatrix}^{\dagger}), \tag{27}$$

where $S \in R^{(n_x+n_d)\times(n_x+n_d+n_y)}$ is an arbitrary matrix.

Remark 3.1. Actually, the matrix S can be chosen according to two criteria. First, the matrix Φ is assumed to be of full rank such that the system matrices of the designed observers are of full rank as well. Second, the first $(n_x + n_d)$ columns of the matrix S is supposed to compose an identity matrix such that the designed observers can have better performance.

3.1. Design of the ETIO based on the MS method

Based on the equation $\Phi E + \Psi \bar{C} = I_{n_x+n_d}$, the descriptor system (23) is equivalently converted to

$$\begin{cases} \bar{x}(k+1) = \Phi\bar{A}\bar{x}(k) + \Phi\bar{B}u(k) + \Phi\bar{J}\omega(k) + \Psi y(k+1), \\ y(k) = \bar{C}\bar{x}(k). \end{cases} \tag{28}$$

In what follows, an ETIO is constructed using the MS method.

$$\begin{cases} \bar{z}(k+1) = \Phi\bar{A}\bar{z}(k) + \Phi\bar{B}u(k) + (\Phi\bar{J})^{+}\bar{\omega}(k) \\ \qquad - (\Phi\bar{J})^{-}\underline{\omega}(k) + \Psi y_b^t(k+1) \\ \qquad + L_1[y_b^t(k) - \bar{C}\bar{x}(k)] + \bar{h}(k), \\ \underline{z}(k+1) = \Phi\bar{A}\underline{z}(k) + \Phi\bar{B}u(k) + (\Phi\bar{J})^{+}\underline{\omega}(k) \\ \qquad - (\Phi\bar{J})^{-}\bar{\omega}(k) + \Psi y_b^t(k+1) \\ \qquad + L_1[y_b^t(k) - \bar{C}\bar{x}(k)] + \underline{h}(k), \end{cases} \tag{29}$$

where $\bar{z}(k)$, $\underline{z}(k)$ are the states of the upper-ETIO and lower-ETIO, respectively, $L_1 \in R^{n_x\times n_y}$ is the observer gain matrix to be designed. Moreover,

$$\begin{cases} \bar{h}(k) = \Psi^{-}e_y^{+}(k+1) + \Psi^{-}\bar{b}(k+1) - \Psi^{+}e_y^{-}(k+1) \\ \qquad + \Psi^{+}\underline{b}(k+1) + L_1^{-}e_y^{+}(k) + L_1^{-}\bar{b}(k) \\ \qquad - L_1^{+}e_y^{-}(k) + L_1^{+}\underline{b}(k), \\ \underline{h}(k) = \Psi^{-}e_y^{-}(k+1) + \Psi^{-}\underline{b}(k+1) - \Psi^{+}e_y^{+}(k+1) \\ \qquad + \Psi^{+}\bar{b}(k+1) + L_1^{-}e_y^{-}(k) + L_1^{-}\underline{b}(k) \\ \qquad - L_1^{+}e_y^{+}(k) + L_1^{+}\bar{b}(k), \end{cases} \tag{30}$$

where $e_y^{-}(k)$ and $e_y^{+}(k)$ are the upper and lower bounds of $e_y(k)$, respectively, $\bar{b}(k)$ and $\underline{b}(k)$ are obtained from Lemma 2.1, L_1 is the observer gain to be determined.

Remark 3.2. The existence of the upper and lower bounds of $e_y(k)$, i.e., $e_y^{-}(k)$ and $e_y^{+}(k)$ are available since the ETM is considered in this paper with the trigger condition $e_y^T(k)e_y(k) < \delta y^T(k)y(k)$. $y^t(k)$ is updated to be equal to $y(k)$ once the condition is violated, which means $e_y(k)$ is set to be 0 and the condition is satisfied again. Therefore, the boundedness of $e_y(k)$ is ensured. Furthermore, the reachable set of $e_y(k)$, i.e., $\mathbf{\Gamma_y}$, can be determined based on $e_y^{-}(k)$ and $e_y^{+}(k)$.

Theorem 3.1. *If there exists a matrix L_1 such that $A - L_1C$ is both Schur and nonnegative, then the inequality*

$$\underline{z}(k) \le \bar{x}(k) \le \bar{z}(k) \tag{31}$$

holds $\forall k \ge 0$ provided that $\underline{z}(0) \le \bar{x}(0) \le \bar{z}(0)$.

The proof of Theorem 3.1 is directly derived from the work of [27], and we just omit it here. The ETIO design method we employ in this subsection is similar to that in [20]. In the next subsection, we present a novel interval estimation approach which is able to remove the restriction that the matrix $A - L_1C$ should be both Schur and nonnegative and moreover, provide higher accuracy in secure estimation.

3.2. Design of the ETIO based on the SM method

In this subsection, secure estimation of $\bar{x}(k)$ is completed by

$$\begin{cases} \bar{x}^{+}(k) = \hat{\bar{x}}(k) + e^{+}(k), \\ \bar{x}^{-}(k) = \hat{\bar{x}}(k) + e^{-}(k), \end{cases} \tag{32}$$

where $\bar{x}^{+}(k)$ and $\bar{x}^{-}(k)$ are upper and lower estimation of $\bar{x}(k)$, $\hat{\bar{x}}(k)$ is the state vector of a Luenberger observer given afterwards, $e^{+}(k)$ and $e^{-}(k)$ are upper and lower bounds of $e(k)$ to be determined by the SM method.

As the first step, we construct a Luenberger observer which has the following form

$$\begin{aligned} \hat{\bar{x}}(k+1) = {} & \Phi\bar{A}\hat{\bar{x}}(k) + \Phi\bar{B}u(k) + L_2[y_b^t(k) - \bar{C}\hat{\bar{x}}(k)] \\ & + \Psi y_b^t(k+1), \end{aligned} \tag{33}$$

where $L_2 \in R^{(n_x+n_d)\times n_y}$ is the gain matrix to be designed. Φ and Ψ are determined by (27). Define $e(k) = \bar{x}(k) - \hat{\bar{x}}(k)$, then it is deduced from (28) and (33) that

$$\begin{aligned} e(k+1) = {} & (\Phi\bar{A} - L_2\bar{C})e(k) + \Phi\bar{J}\omega(k) - L_2e_y(k) \\ & - \Psi e_y(k+1) - L_2b(k) - \Psi b(k+1). \end{aligned} \tag{34}$$

For simplicity, the first equation of (23) and (34) are rewritten as

$$\bar{x}(k+1) = \Phi\bar{A}\bar{x}(k) + \Psi y(k+1) + \hat{B}g(k), \tag{35}$$

$$e(k+1) = (\Phi\bar{A} - L_2\bar{C})e(k) + L_{21}e_y^*(k) + L_{22}g(k), \tag{36}$$

where

$$\begin{aligned} g(k) &= \begin{bmatrix} b^T(k) & b^T(k+1) & \omega^T(k) & u^T(k) \end{bmatrix}^T, \\ e_y^*(k) &= \begin{bmatrix} e_y^T(k) & e_y^T(k+1) \end{bmatrix}^T, \\ \hat{B} &= \begin{bmatrix} 0 & 0 & \Phi\bar{J} & \Phi\bar{B} \end{bmatrix}, \\ L_{21} &= \begin{bmatrix} -L_2 & -\Psi \end{bmatrix}, \\ L_{22} &= \begin{bmatrix} -L_2 & -\Psi & \Phi\bar{J} & 0 \end{bmatrix}. \end{aligned} \tag{37}$$

In addition, (34) can also be rewritten as

$$e(k+1) = A_e e(k) + F_e v(k), \tag{38}$$

where

$$\begin{aligned} A_e &= \Phi\bar{A} - L_2\bar{C}, \\ F_e &= \begin{bmatrix} \Phi\bar{J} & -L_2 & -\Psi & -L_2 & -\Psi \end{bmatrix}, \\ v(k) &= \\ &\quad \begin{bmatrix} \omega^T(k) & e_y^T(k) & e_y^T(k+1) & b^T(k) & b^T(k+1) \end{bmatrix}^T. \end{aligned} \tag{39}$$

Remark 3.3. From Assumption 2.1 and Lemma 2.1, we know that $\omega(k)$ and $b(k)$ are both bounded vectors. In addition, $u(k)$ is a predetermined bounded vector. Hence, $g(k)$ is also a bounded vector, i.e.,

$$\|g(k)\|^2 \le g^*, \tag{40}$$

where g^* is a positive constant.

Denote $\xi(k) = \begin{bmatrix} \bar{x}^T(k) & e^T(k) \end{bmatrix}^T$, according to (23), (35) and (36), we have

$$\begin{cases} \xi(k+1) = \tilde{A}\xi(k) + L_2^* e_y^*(k) + \tilde{B}g(k) \\ \qquad\qquad + \Psi^* y(k+1), \\ y(k) = \tilde{C}\xi(k), \end{cases} \tag{41}$$

where

$$\begin{aligned} \tilde{A} &= \begin{bmatrix} \Phi\bar{A} & 0 \\ 0 & \Phi\bar{A} - L_2\bar{C} \end{bmatrix}, \\ \tilde{B} &= \begin{bmatrix} \hat{B} \\ L_{22} \end{bmatrix}, L_2^* = \begin{bmatrix} 0 \\ L_{21} \end{bmatrix}, \\ \Psi^* &= \begin{bmatrix} \Psi \\ 0 \end{bmatrix}, \tilde{C} = \begin{bmatrix} \bar{C} & 0 \end{bmatrix}. \end{aligned} \tag{42}$$

In what follows, the notion of input-to-state stable (ISS) and H_∞ robust observer are introduced. By seeking the sufficient conditions for error dynamic Eq. (34) to be both ISS and H_∞ robust and transforming it into LMI problems, the gain matrix L_2 can be determined.

Definition 3.1 ([28]). A K-class function ϵ is a function that satisfies continuity and strictly increasing property with initial condition $\epsilon(0) = 0$. A KL-class function $\varepsilon : R^+ \times Z^+$ is a function satisfying that $\forall k \ge 0$, $\varepsilon(\cdot, k)$ is a K-class function, $\varepsilon(s, \cdot)$ is decreasing and $\varepsilon(s, k) \to 0$ as $k \to \infty$.

Definition 3.2 ([28]). Given initial condition $e(0)$, the error system (34) with trigger condition (2) is ISS with injected bias $b(k)$ and external disturbance $\omega(k)$, if there exist a KL-class function ε and a K-class function ϵ such that the following inequality holds

$$\|e(k)\| < \varepsilon(\|e(0)\|, k) + \epsilon(\|g[0, k]\|). \tag{43}$$

Definition 3.3 ([1]). The Luenberger observer (33) is H_∞ robust if the following conditions hold for (38),
(1) $v(k) = 0$, $e(k) \to 0$ as $k \to \infty$,
(2) $v(k) \ne 0$, when $e(0) = 0$, it holds that

$$\sum_{k=0}^{\infty} e^T(k)e(k) \le \eta \sum_{k=0}^{\infty} v^T(k)v(k) \tag{44}$$

where $\eta > 0$ stands for the disturbance attenuate level, and $v(k)$ is defined in (38).

Theorem 3.2. *Given positive constants α_i $(i = 1, 2, \ldots, 6)$ and event-triggered condition (2), if there exist matrices $P \succ 0$, $Q \succ 0$, scalars $\gamma_1 > 0$, $\gamma_2 > 0$ which satisfy $0 < \gamma_2/(1-\gamma_1) < 1$ and scalars ξ, η, such that*

$$\begin{bmatrix} \gamma_1 P & \Theta_1 \\ \Theta_1^T & P^{-1} \end{bmatrix} \succ 0, \tag{45}$$

$$\begin{bmatrix} -\gamma_2 P & \Theta_2 \\ \Theta_2^T & -P^{-1} \end{bmatrix} \prec 0, \tag{46}$$

$$\begin{bmatrix} I - \xi Q & * & * & * & * & * & * \\ 0 & -\eta I & * & * & * & * & * \\ 0 & 0 & -\eta I & * & * & * & * \\ 0 & 0 & 0 & -\eta I & * & * & * \\ 0 & 0 & 0 & 0 & -\eta I & * & * \\ 0 & 0 & 0 & 0 & 0 & -\eta I & * \\ Q\Phi\bar{A} - Y\bar{C} & Q\Phi\bar{J} & -Y & -Q\Psi & -Y & -Q\Psi & -Q \end{bmatrix} \prec 0 \tag{47}$$

where

$$\begin{aligned} \Theta_1 &= -\sqrt{\delta(1+\alpha_3+\alpha_5+\alpha_6)}\tilde{C}^T\Psi^{*T}, \\ \Theta_2 &= \sqrt{1 + \frac{1}{\alpha_1} + \frac{1}{\alpha_2} + \frac{1}{\alpha_3}}\tilde{A}^T, \end{aligned} \tag{48}$$

then the system (41) is ISS and the error dynamics (34) is H_∞ robust. Moreover, the matrix L_2 can be determined by $L_2 = Q^{-1}Y$ and the error dynamics can reach its maximum robustness by minimizing the scalar η.

The following lemma is introduced before the proof of Theorem 3.2 is presented.

Lemma 3.2 ([29]). *Given matrices U, V with appropriate dimensions and a positive constant α, it holds that*

$$U^TV + V^TU \le \frac{1}{\alpha}U^TPU + \alpha V^TP^{-1}V, \tag{49}$$

where $P \succ 0$.

The proof of Theorem 3.2 will be divided into two parts, i.e., the proof of the input-to-state stability and the proof of the H_∞ robustness.

Proof. (i) The proof of input-to-state stability.

Choose the Lyapunov candidate function $V(k) = \xi^T(k)P\xi(k)$ and take the difference along the dynamics (41), it yields that

$$\begin{aligned} &\Delta(k) \\ =&V(k+1) - V(k) \\ =&\xi^T(k+1)P\xi(k+1) - \xi^T(k)P\xi(k) \\ =&\xi^T(k)[\tilde{A}^TP\tilde{A} - P]\xi(k) + e_y^{*T}(k)L_2^{*T}PL_2^*e_y^*(k) \\ &+ g^T(k)\tilde{B}^TP\tilde{B}g(k) + y^T(k+1)\Psi^{*T}P\Psi^*y(k+1) \\ &+ \sum_{i=1}^{6}[F_i(k) + F_i^T(k)], \end{aligned} \tag{50}$$

where

$$\begin{aligned}
F_1(k) =&\xi^T(k)\tilde{A}^T P L_2^* e_y^*(k),\\
F_2(k) =&\xi^T(k)\tilde{A}^T P\tilde{B}g(k),\\
F_3(k) =&\xi^T(k)\tilde{A}^T P\Psi^* y(k+1),\\
F_4(k) =&e_y^{*T}(k)L_2^{*T}P\tilde{B}g(k),\\
F_5(k) =&e_y^{*T}(k)L_2^{*T}P\Psi^* y(k+1),\\
F_6(k) =&g^T(k)\tilde{B}^T\tilde{B}^T P\Psi^* y(k+1).
\end{aligned} \tag{51}$$

It is derived from Lemma 3.2 that

$$\begin{aligned}
F_1(k)+F_1^T(k) \le&(1/\alpha_1)\xi^T(k)\tilde{A}^T P\tilde{A}\xi(k)\\
&+\alpha_1 e_y^{*T}(k)L_2^{*T}PL_2^* e_y^*(k),\\
F_2(k)+F_2^T(k) \le&(1/\alpha_2)\xi^T(k)\tilde{A}^T P\tilde{A}\xi(k)\\
&+\alpha_2 g^T(k)\tilde{B}^T P\tilde{B}g(k),\\
F_3(k)+F_3^T(k) \le&(1/\alpha_3)\xi^T(k)\tilde{A}^T P\tilde{A}\xi(k)\\
&+\alpha_3 y^T(k+1)\Psi^{*T}P\Psi^* y(k+1),\\
F_4(k)+F_4^T(k) \le&(1/\alpha_4)e_y^{*T}(k)L_2^{*T}PL_2^* e_y^*(k)\\
&+\alpha_4 g^T(k)\tilde{B}^T P\tilde{B}g(k),
\end{aligned} \tag{52}$$

$$\begin{aligned}
F_5(k)+F_5^T(k) \le&(1/\alpha_5)e_y^{*T}(k)L_2^{*T}PL_2^* e_y^*(k)\\
&+\alpha_5 y^T(k+1)\Psi^{*T}P\Psi^* y(k+1),\\
F_6(k)+F_6^T(k) \le&(1/\alpha_6)g^T(k)\tilde{B}^T P\tilde{B}g(k)\\
&+\alpha_6 y^T(k+1)\Psi^{*T}P\Psi^* y(k+1).
\end{aligned} \tag{53}$$

Thus,

$$\begin{aligned}
&\Delta(k)\\
\le&\xi^T(k)[(1+1/\alpha_1+1/\alpha_2+1/\alpha_3)\tilde{A}^T P\tilde{A}-P]\xi(k)\\
+&e_y^{*T}(k)[(1+\alpha_1+1/\alpha_4+1/\alpha_5)L_2^{*T}PL_2^*]e_y^*(k)\\
+&g^T(k)[(1+\alpha_2+\alpha_4+1/\alpha_6)\tilde{B}^T P\tilde{B}]g(k)\\
+&y^T(k+1)[(1+\alpha_3+\alpha_5+\alpha_6)\Psi^{*T}P\Psi^*]y(k+1).
\end{aligned} \tag{54}$$

Note that the event-triggered condition (2) can be recast as

$$\begin{aligned}
&e_y^{*T}(k)e_y^*(k)\\
<&\delta y^T(k)y(k)+\delta y^T(k+1)y(k+1)\\
=&\delta\xi^T(k)\tilde{C}^T\tilde{C}\xi(k)+\delta\xi^T(k+1)\tilde{C}^T\tilde{C}\xi(k+1),
\end{aligned} \tag{55}$$

where $\tilde{C}=\begin{bmatrix}\bar{C} & 0_{n_x}\end{bmatrix}$, hence

$$\begin{aligned}
&\xi^T(k+1)[P-\delta(1+\alpha_3+\alpha_5+\alpha_6)\tilde{C}^T\Psi^{*T}P\Psi^*\tilde{C}\\
&-\delta(1+\alpha_1+1/\alpha_4+1/\alpha_5)\tilde{C}^T L_2^{*T}PL_2^*\tilde{C}]\xi(k+1)\le\\
&\xi^T(k)[(1+1/\alpha_1+1/\alpha_2+1/\alpha_3)\tilde{A}^T P\tilde{A}\\
&+\delta(1+\alpha_1+1/\alpha_4+1/\alpha_5)\tilde{C}^T L_2^{*T}PL_2^*\tilde{C}]\xi(k)\\
&+g^T(k)[(1+\alpha_2+\alpha_4+1/\alpha_6)\tilde{B}^T P\tilde{B}]g(k).
\end{aligned} \tag{56}$$

By applying Schur complement and in consideration of $\tilde{C}L_2^*=\mathbf{0}$, it indicates from (45) and (56) that

$$\begin{aligned}
&(1-\gamma_1)\xi^T(k+1)P\xi(k+1)\le\gamma_2\xi^T(k)P\xi(k)\\
&+g^T(k)[(1+\alpha_2+\alpha_4+1/\alpha_6)\tilde{B}^T P\tilde{B}]g(k),
\end{aligned} \tag{57}$$

i.e.,

$$V(k+1)\le\gamma V(k)+\Pi(k), \tag{58}$$

where $0<\gamma=\gamma_2/(1-\gamma_1)<1$, $\Pi(k)=(1/(1-\gamma_1))g^T(k)[(1+\alpha_2+\alpha_4+1/\alpha_6)\tilde{B}^T P\tilde{B}]g(k)$. By iteration, one has

$$\begin{aligned}
V(k)<&\gamma^k V(0)+\sum_{j=1}^{k}\gamma^{j-1}\Pi(k-j)\\
<&\gamma^k V(0)+\frac{(1-\gamma^k)\bar{\Pi}g^*}{1-\gamma},
\end{aligned} \tag{59}$$

where $\bar{\Pi}=(1+\alpha_2+\alpha_4+1/\alpha_6)\lambda_{max}(\tilde{B}^T P\tilde{B})$ and g^* is introduced in (40). The proof is completed here.

(ii) The proof of robustness.

This part of proof can be referred to [1], we just omit it here.

Remark 3.4. Note that the matrix L_2 exists both in (46) and (47), a possible approach to solve these LMIs is presented in the following steps,

Step 1: Solve (47) and obtain L_2;

Step 2: Substitute L_2 into (46) and obtain P;

Step 3: Substitute P into (45) and verify the positivity of (45).

Or

Step 1: Solve (47) and obtain L_2;

Step 2: Solve (45) and obtain P;

Step 3: Substitute P and L_2 into (46) and verify the negativity of (46).

In what follows, the SM method is applied to obtain the upper and lower estimation of error dynamics (34) and subsequently on the basis of (32), event-triggered secure estimation of CPS with UIs is accomplished.

Theorem 3.3. *For CPS (1) subject to stealthy deception attacks, under event-triggered condition (2), the interval estimation can be accomplished on the basis of (32) considering that $\hat{\bar{x}}(0)=p_0$, where $e^+(k)$ and $e^-(k)$ are determined by*

$$\begin{aligned}
[e^-(k),e^+(k)] =&\mathcal{H}((\Phi\bar{A}-L_2\bar{C})^k\langle 0,Q_0\rangle)\\
&\oplus\bigoplus_{i=0}^{k-1}\mathcal{H}((\Phi\bar{A}-L_2\bar{C})^i(-(L_2+\Psi)\mathbf{\Gamma_y}))\\
&\oplus\bigoplus_{i=0}^{k}\mathcal{H}((\Phi\bar{A}-L_2\bar{C})^i(-(L_2+\Psi)\mathbf{\Lambda}))\\
&\oplus\bigoplus_{i=0}^{k}\mathcal{H}((\Phi\bar{A}-L_2\bar{C})^i(\Phi\bar{B}\mathbf{W})),
\end{aligned} \tag{60}$$

where $\mathbf{\Gamma_y}$ represents the reachable set of $e_y(k)$ that can be determined according to Remark 3.2, $\mathbf{\Lambda}$ is reachable set of $b(k)$ introduced in Lemma 2.1 and $\mathbf{W}$ is defined in (14).

Proof. Recall that

$$\begin{aligned}
&e(k+1)\\
=&(\Phi\bar{A}-L_2\bar{C})e(k)-L_2e_y(k)-\Psi e_y(k+1)\\
&-L_2b(k)-\Psi b(k+1)+\Phi\bar{B}\omega(k).
\end{aligned} \tag{61}$$

By iteration, it follows from (61) that

$$\begin{aligned} & e(k+1) \\ =&(\Phi\bar{A}-L_2\bar{C})^{k+1}e(0)+\sum_{i=0}^{k}(\Phi\bar{A}-L_2\bar{C})^{i}\Phi\bar{B}\omega(k-i) \\ &-\sum_{i=0}^{k}(\Phi\bar{A}-L_2\bar{C})^{i}L_2[e_y(k-i)+b(k-i)] \\ &-\sum_{i=0}^{k}(\Phi\bar{A}-L_2\bar{C})^{i}\Psi[e_y(k+1-i)+b(k+1-i)]. \end{aligned} \tag{62}$$

Define $\Omega(k)$ as the reachable set of $e(k)$, since $\hat{\bar{x}}(0)=p_0$, we have $e(0)\in\langle 0, Q_0\rangle$, consequently, we have

$$\begin{aligned} \Omega(k) =&(\Phi\bar{A}-L_2\bar{C})^{k}\langle 0, Q_0\rangle \\ &\oplus\bigoplus_{i=0}^{k-1}(\Phi\bar{A}-L_2\bar{C})^{i}(-(L_2+\Psi)\mathbf{\Gamma_y}) \\ &\oplus\bigoplus_{i=0}^{k-1}(\Phi\bar{A}-L_2\bar{C})^{i}(-(L_2+\Psi)\mathbf{\Lambda}) \\ &\oplus\bigoplus_{i=0}^{k-1}(\Phi\bar{A}-L_2\bar{C})^{i}(\Phi\bar{B}\mathbf{W}). \end{aligned} \tag{63}$$

From Property 2.1 and (63), the interval hull of $\Omega(k)$ can be computed by

$$\begin{aligned} [e^{-}(k), e^{+}(k)] =&\mathcal{H}((\Phi\bar{A}-L_2\bar{C})^{k}\langle 0, Q_0\rangle) \\ &\oplus\bigoplus_{i=0}^{k-1}\mathcal{H}((\Phi\bar{A}-L_2\bar{C})^{i}(-(L_2+\Psi)\mathbf{\Gamma_y})) \\ &\oplus\bigoplus_{i=0}^{k}\mathcal{H}((\Phi\bar{A}-L_2\bar{C})^{i}(-(L_2+\Psi)\mathbf{\Lambda})) \\ &\oplus\bigoplus_{i=0}^{k}\mathcal{H}((\Phi\bar{A}-L_2\bar{C})^{i}(\Phi\bar{B}\mathbf{W})). \end{aligned} \tag{64}$$

This completes the proof.

Remark 3.5. The procedure of event-triggered secure estimation for CPSs subject to UIs is summarized as the following Algorithm.

Algorithm 1: Algorithm for ETIO design for CPSs subject to UIs and stealthy attacks

Input: A, B, C, D, F, J, p_0, Q_0, δ, $\alpha_i(i=1,\ldots,6)$, $u(k)$, $\mathbf{W}$;
Output: $\bar{x}_k$, $\underline{x}_k$
1: **Augment the original system** (1) **into the descriptor system** (23);
2: **Given a scalar** δ, **according to the trigger condition** (2), **obtain** $y^t(k)$ **and** $\mathbf{\Gamma_y}$;
3: **Given zonotope W and matrices** A, B, C, Q_0
4: **do**
5: $\mathcal{B}=CA^k\langle 0, 2Q_0\rangle\oplus\bigoplus_{i=0}^{k-1}\mathcal{H}(2CA^iB\mathbf{W})$;
6: **Output**: $\mathcal{B}$;
7: **Select an appropriate matrix** S **according to** Remark 3.1, then obtain Φ and Ψ according **to** (27) ;
8: **Solve LMI** (45)–(46);
9: **Output:** η, P, Q, Y;
10: **do**
11: $L_2=Q^{-1}Y$;
12: **Given initial conditions:**
$\hat{\bar{x}}_0=p_0$, $[e^{-}(0), e^{+}(0)]=\mathcal{H}(\langle 0, Q_0\rangle)$;
13: **for** $k\geq 0$, **do**
14: $\hat{\bar{x}}(k+1)=\Phi\bar{A}\hat{\bar{x}}(k)+\Phi\bar{B}u(k)+L_2[y_b^t(k)-\bar{C}\hat{\bar{x}}(k)]$
$+\Psi y_b^t(k+1)$;
15: $[e^{-}(k), e^{+}(k)]=\mathcal{H}((\Phi\bar{A}-L_2\bar{C})^{k}\langle 0, Q_0\rangle)$
$\oplus\bigoplus_{i=0}^{k-1}\mathcal{H}((\Phi\bar{A}-L_2\bar{C})^{i}(-(L_2+\Psi)\mathbf{\Gamma_y}))$
$\oplus\bigoplus_{i=0}^{k}\mathcal{H}((\Phi\bar{A}-L_2\bar{C})^{i}(-(L_2+\Psi)\mathcal{B}))$
$\oplus\bigoplus_{i=0}^{k}\mathcal{H}((\Phi\bar{A}-L_2\bar{C})^{i}(\Phi\bar{B}\mathbf{W}))$;
16: $\bar{x}^{+}(k)=\hat{\bar{x}}(k)+e^{+}(k)$, $\bar{x}^{-}(k)=\hat{\bar{x}}(k)+e^{-}(k)$;
17: **end for**

Remark 3.6. The SM method can be regarded as an improvement of the MS method employed in this paper and in [5,6]. For the MS method, a gain matrix with specific property is essential, whose existence depends on the structure of system matrix and output matrix. Although coordinate transformation was utilized in [30, 31] to reduce its restrictions, more conservatism is introduced and the construction of IOs seems more complicated. Compared to the MS method, the SM method can be applied without pre-conditions. Additionally, H_∞ technique can be combined with Luenberger observer design to guarantee the robustness of the IOs. Moreover, the SM method is characterized by higher precision in SE, which is verified theoretically and practically by Tang et al. [32].

4. Illustrative examples

4.1. Example 1

Example 1 is an original numerical experiment. According to Algorithm 1, the input parameters are chosen as:

$$\begin{aligned} &A=\begin{bmatrix}0.1841 & 0 & 0.0419\\ 0 & 0.3888 & 0\\ 0 & 0.1785 & 0.3581\end{bmatrix}, J=\begin{bmatrix}0.7\\ 0\\ 0.5\end{bmatrix}, C=\begin{bmatrix}1 & 0 & 1\end{bmatrix}, \\ &D=\begin{bmatrix}0\\ 1\\ 0.2\end{bmatrix}, F=0.3, p_0=\begin{bmatrix}0 & 0 & 0\end{bmatrix}^T, Q_0=\begin{bmatrix}0.5 & & \\ & 0.5 & \\ & & 0.5\end{bmatrix}, \\ &W=0.5, u(k)=2, d(k)=2(1-e^{-k}), \delta=0.15, \\ &\alpha_i=i\ (i=1,2,\ldots,6), \gamma_1=0.2, \gamma_2=0.5, \\ &0<\gamma=\gamma_2/(1-\gamma_1)=0.5/(1-0.2)=0.625<1. \end{aligned} \tag{65}$$

The following steps are taken to obtain the outputs $\bar{x}_k$ and $\underline{x}_k$:

1: Transform the original system into a descriptor system modeled by:

$$\begin{aligned} &E=\begin{bmatrix}1 & 0 & 0 & 0\\ 0 & 1 & 0 & 0\\ 0 & 0 & 1 & 0\\ 0 & 0 & 0 & 0\end{bmatrix}, \bar{A}=\begin{bmatrix}0.1841 & 0 & 0.0419 & 0\\ 0 & 0.3888 & 0 & 1\\ 0 & 0.1785 & 0.3581 & 0.2\\ 0 & 0 & 0 & 0\end{bmatrix}, \\ &\bar{B}=\begin{bmatrix}1\\ 1\\ 1\\ 0\end{bmatrix}, \bar{J}=\begin{bmatrix}0.7\\ 0\\ 0.5\\ 0\end{bmatrix}, \bar{C}=\begin{bmatrix}1 & 0 & 1 & 0.3\end{bmatrix}. \end{aligned} \tag{66}$$

2: According to the given scalar $\delta=0.5$, we can form the trigger condition (2), then obtain the triggering instants t_i, the transmitted data $y^t(k)$ and the reachable set of e_y. Consequently, the triggering instants and the intervals between two successive sensor events are depicted in Fig. 2.

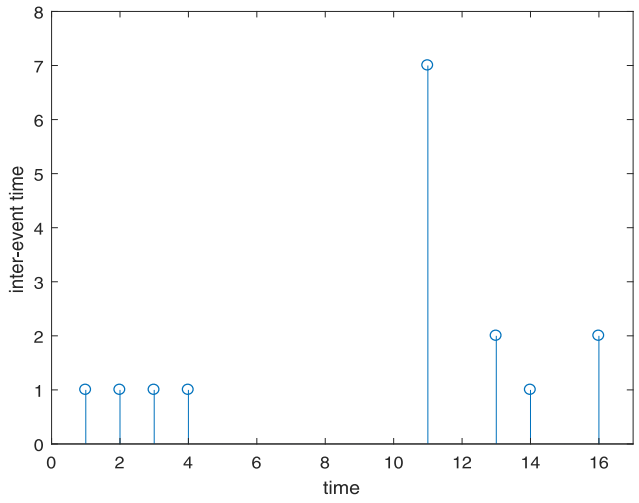

Fig. 2. Sequence of event-triggering intervals.

Table 1

	Aver_w	Event-triggered condition
The method in [20]	2.5857	$e_y^T(k)Q_k e_y(k) < \rho_k y^T(k)Q_k y(k)$
The proposed method	0.5785	$e_y^T(k)e_y(k) < \delta y^T(k)y(k)$

3: Given zonotope $\mathbf{W}$ and matrices A, B, C, Q_0, calculate the reachable set of b_k by

$$\mathcal{B} = CA^k\langle 0, 2Q_0\rangle \oplus \bigoplus_{i=0}^{k-1} \mathcal{H}(2CA^iB\mathbf{W}). \tag{67}$$

4. Select $S = \begin{bmatrix}\mathbf{I_4} & \mathbf{0}\end{bmatrix} \in R^{4\times 5}$, then according to (27), one obtains

$$\begin{bmatrix}\Phi & \Psi\end{bmatrix} = \begin{bmatrix} 1 & 0 & 0 & 0 & 0 \\ 0 & 1 & 0 & 0 & 0 \\ 0 & 0 & 1 & 0 & 0 \\ 0 & 0 & 1 & 0 & 0 \\ -\frac{10}{3} & 0 & -\frac{10}{3} & 1 & \frac{10}{3} \end{bmatrix}. \tag{68}$$

5. Based on the given scalars γ_1, γ_2, solve LMIs (45)–(47), a feasible solution is

$$\eta = 110.3406, P = \begin{bmatrix} P_1 & \mathbf{0} \\ \mathbf{0} & P_2 \end{bmatrix} \times 10^3, L_2 = \begin{bmatrix} -0.0086 \\ 2.1976 \\ 0.3163 \\ -1.0240 \end{bmatrix}, \tag{69}$$

where

$$P_1 = \begin{bmatrix} 4.4359 & 0 & -0.2324 & -0.1189 \\ 0 & 4.6683 & 0 & 0 \\ -0.2324 & 0 & 4.4359 & -0.1189 \\ -0.1189 & 0 & -0.1189 & 4.0691 \end{bmatrix}$$
$$P_2 = \begin{bmatrix} 4.6683 & 0 & 0 & 0 \\ 0 & 4.6683 & 0 & 0 \\ 0 & 0 & 4.6683 & 0 \\ 0 & 0 & 0 & 4.6683 \end{bmatrix}. \tag{70}$$

6. With the initial conditions

$$\hat{\bar{x}}_0 = p_0, [e^-(0), e^+(0)] = \mathcal{H}(\langle 0, Q_0\rangle), \tag{71}$$

and the observer gain matrix L_2, construct the Luenberger observer by

$$\hat{\bar{x}}(k+1) = \Phi\bar{A}\hat{\bar{x}}(k) + \Phi\bar{B}u(k) + L_2[y_b^t(k) - \bar{C}\hat{\bar{x}}(k)]. \tag{72}$$

7. Calculate the interval hull of $e(k)$ by

$$\begin{aligned}[e^-(k), e^+(k)] = {} & \mathcal{H}((\Phi\bar{A} - L_2\bar{C})^k\langle 0, Q_0\rangle) \\ & \oplus \bigoplus_{i=0}^{k-1} \mathcal{H}((\Phi\bar{A} - L_2\bar{C})^i(-(L_2+\Psi)\mathbf{\Gamma_y})) \\ & \oplus \bigoplus_{i=0}^{k} \mathcal{H}((\Phi\bar{A} - L_2\bar{C})^i(-(L_2+\Psi)\mathcal{B})) \\ & \oplus \bigoplus_{i=0}^{k} \mathcal{H}((\Phi\bar{A} - L_2\bar{C})^i(\Phi\bar{B}\mathbf{W})).\end{aligned} \tag{73}$$

8. Accomplish interval estimation by

$$\bar{x}^+(k) = \hat{\bar{x}}(k) + e^+(k), \bar{x}^-(k) = \hat{\bar{x}}(k) + e^-(k) \tag{74}$$

Based on the steps shown above, the simulation results are presented in Fig. 3.

It can be concluded from Figs. 3(b)–3(d) that due to the convergence of $e(k)$ obtained by the SM method, the proposed method provides gradually tighter intervals over time. To further reveal the superiority of the method proposed in this paper, comparisons with the IO constructed in [20] are provided. A more complex event-triggered protocol is proposed in [20] and it is characterized by decreasing triggering frequency over time. However, the IOs in [20] are constructed via positive system theory, which is able to guarantee nonnegativity, but not estimation accuracy. In order to evaluate the accuracy of the two methods, Table 1 is presented. Define the performance measures as *Aver_w*, which indicates the average value of the interval width, i.e.

$$Aver\_w = \frac{E[x_1^+ - x_1^-] + E[x_2^+ - x_2^-] + E[x_3^+ - x_3^-]}{3}, \tag{75}$$

or,

$$Aver\_w = \frac{E[\bar{z}_1 - \underline{z}_1] + E[\bar{z}_2 - \underline{z}_2] + E[\bar{z}_3 - \underline{z}_3]}{3}, \tag{76}$$

where $E[\cdot]$ stands for the mean value.

Figs. 3(b)–3(d) and Table 1 indicate that the proposed method provides tighter bounds compared to the method in [20]. Moreover, the method in [20] requires that there exists matrices L_k such that $A_k - L_kC_k$ are nonnegative matrices. However, if matrices A_k are not in some specific form, then it is impossible to find such matrices L_k. In comparison with that, the constrained condition of this paper is that the matrix equation $\Phi E + \Psi\bar{C} = I$ is supposed to be solvable, which is not a strict condition in general.

Remark 4.1. Two reasons are able to explain why the proposed method is characterized by higher precision in SE: (i) An essential step to construct ETIO for CPSs subject to UIs and stealthy attack is the reachable set calculation of the injected bias b_k using SM method, which is shown in Steps 5–7 in Algorithm 1. The similar treatment is employed by [8,20,21], in which the bounds of the attack signal are estimated by constructing IOs using the MS method; (ii) As the first step of the SM method, the design of the Luenberger observer is combined with the H_∞ technique to optimize the robustness of the observer against disturbances. Thus, the effect of the disturbances on the performance of ETIO is weakened. To further reveal the influence of the two factors, ablation experiments are carried out in what follows.

Repeat Step 1–Step 8 without regard to the reachable set calculation of the injected bias b_k, i.e., skip Step 3 and reformulate

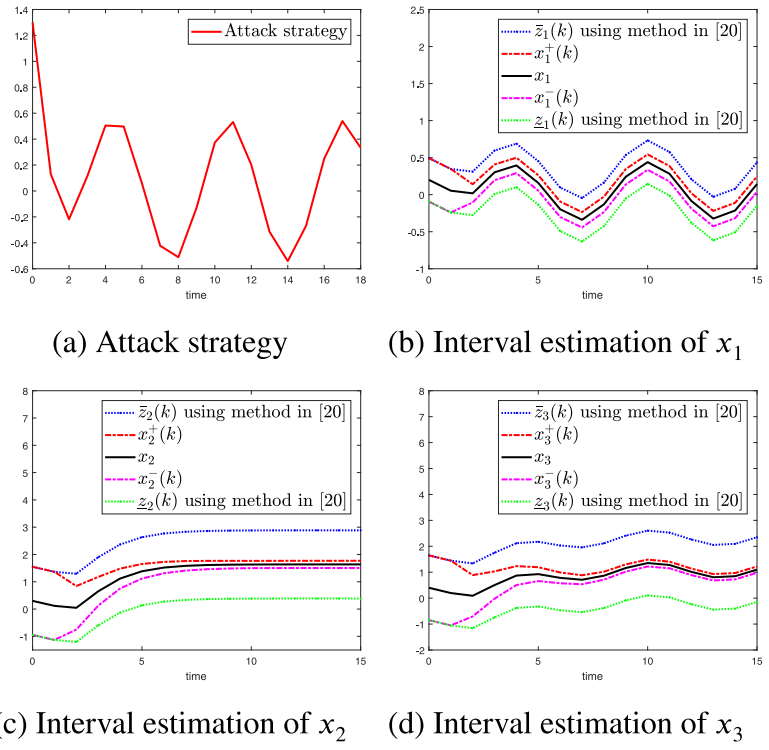

(a) Attack strategy (b) Interval estimation of x_1

(c) Interval estimation of x_2 (d) Interval estimation of x_3

Fig. 3. Results of Example 1.

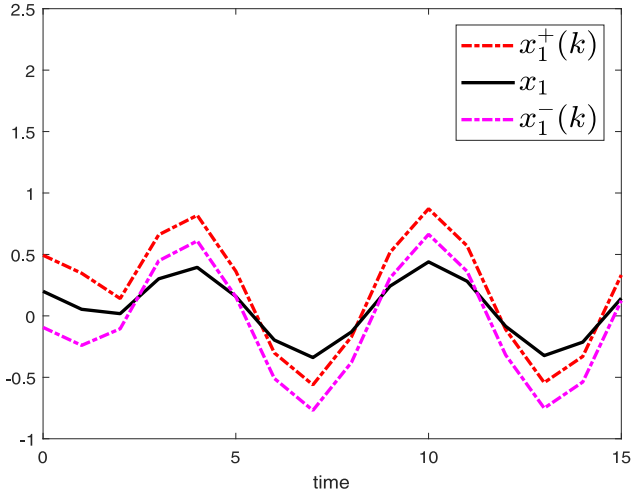

Fig. 4. Interval estimation of x_1 ignoring calculation of $\mathcal{B}$.

(73) in Step 7 as

$$\begin{aligned}[e^-(k), e^+(k)] = {} & \mathcal{H}((\Phi\bar{A} - L_2\bar{C})^k\langle 0, Q_0\rangle) \\ & \oplus \bigoplus_{i=0}^{k-1} \mathcal{H}((\Phi\bar{A} - L_2\bar{C})^i(-(L_2 + \Psi)\mathbf{\Gamma_y})) \\ & \oplus \bigoplus_{i=0}^{k} \mathcal{H}((\Phi\bar{A} - L_2\bar{C})^i(\Phi\bar{B}\mathbf{W})).\end{aligned} \tag{77}$$

The results are shown in Fig. 4, which implies that ignoring calculation of $\mathcal{B}$ may cause failure of SE.

In what follows, the Luenberger observer in Step 6 is reconstructed without minimization of η, that is, the H_∞ technique is avoided. The results of Step 5 are updated to

$$\eta = 174.3406 > 110.3406,$$

$$P = \begin{bmatrix} P_1 & \mathbf{0} \\ \mathbf{0} & P_2 \end{bmatrix} \times 10^3, L_2 = \begin{bmatrix} 0.0489 \\ 1.3674 \\ 0.2972 \\ -1.1231 \end{bmatrix}, \tag{78}$$

where

$$P_1 = \begin{bmatrix} 4.4359 & 0 & -0.2324 & -0.1189 \\ 0 & 4.6683 & 0 & 0 \\ -0.2324 & 0 & 4.4359 & -0.1189 \\ -0.1189 & 0 & -0.1189 & 4.0691 \end{bmatrix},$$

$$P_2 = \begin{bmatrix} 4.6683 & 0 & 0 & 0 \\ 0 & 4.6683 & 0 & 0 \\ 0 & 0 & 4.6683 & 0 \\ 0 & 0 & 0 & 4.6683 \end{bmatrix}. \tag{79}$$

Figs. 5(a)–5(c) depicts the effect of H_∞ technique, from which we can conclude that SE can be accomplished without consideration of H_∞, however, the performance of the ETIO is degraded due to the disturbances.

4.2. Example 2

Example 2 is a practical example borrowed from [33]. As the physical resource layer in a smart factory, a two-tank system is depicted in Figs. 6(a)–6(b). The two-tank system is composed of two tanks, a pump, a water basin and several water pipelines, as shown in Fig. 6(a). The water level of Tank 1 is affected by the manual valve placed between Tank 1 and Tank 2. And the water level of Tank 2 is affected by the pump together with the manual valve.

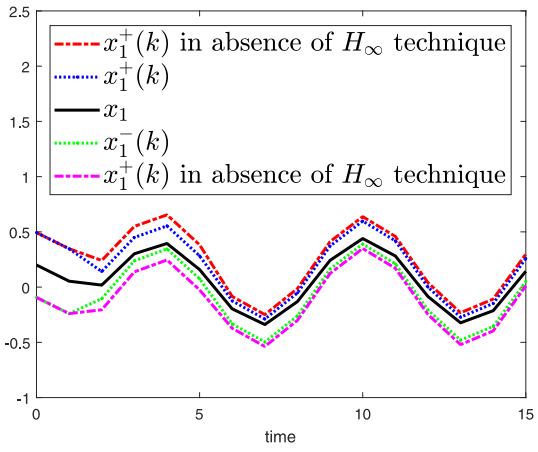

(a) Interval estimation of x_1 in presence/absence of H_∞ technique

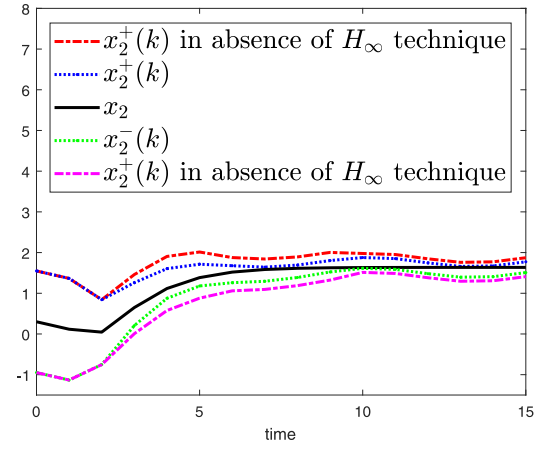

(b) Interval estimation of x_2 in presence/absence of H_∞ technique

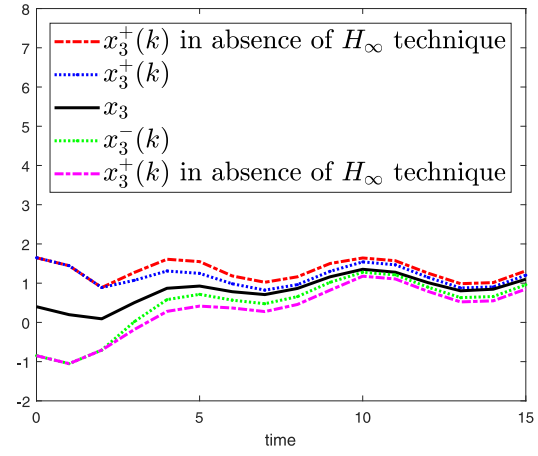

(c) Interval estimation of x_3 in presence/absence of H_∞ technique

Fig. 5. The effect of H_∞ technique.

The mathematical model of the system is

$$\begin{aligned}\frac{dh_1^\circ(t)}{dt} &= -\frac{a_1}{A_1}\sqrt{2gh_1^\circ(t)} + \frac{a_2}{A_1}\sqrt{2gh_1^\circ(t)} + \frac{\gamma K_p}{A_1}\omega(t)\\ \frac{dh_2^\circ(t)}{dt} &= -\frac{a_2}{A_2}\sqrt{2gh_2^\circ(t)} + \frac{(1-\gamma)K_p}{A_2}\nu^\circ(t)\end{aligned} \tag{80}$$

(a) Physical picture of the two-tank system

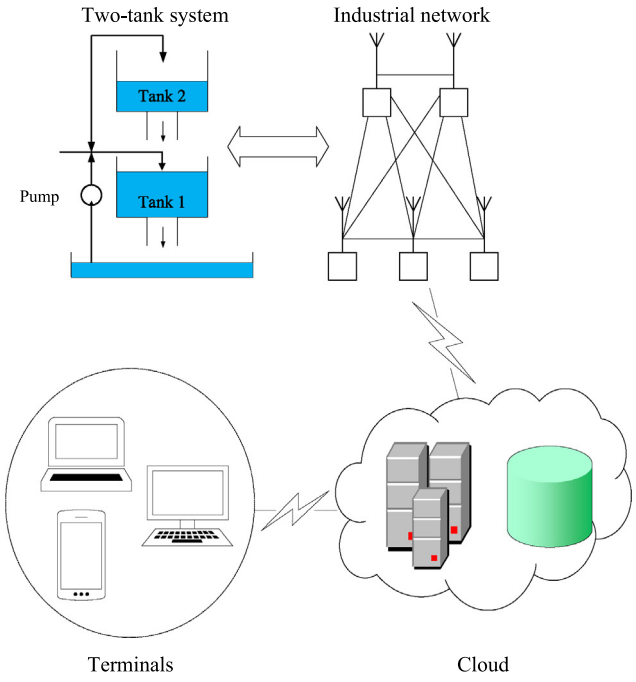

(b) A basic framework of the smart factory

Fig. 6. The two-tank system.

The parameters in (80) are explained in Table 2.

Based on the work of [33], the state-space dynamics of (80) in discrete form is

$$\begin{cases} h(k+1) = Ah(k) + Bu(k) + J\omega(k) + Dd(k), \\ y(k) = Ch(k) + Fd(k), \end{cases} \tag{81}$$

where $h(k) = \begin{bmatrix} h_1(k) & h_2(k) \end{bmatrix}$ represents the vector of the water levels of two tanks. According to Algorithm 1, the input

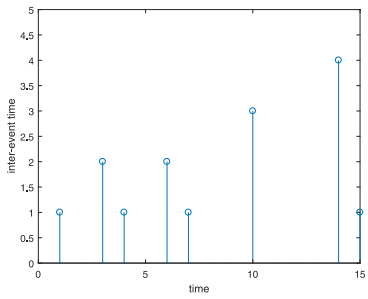

(a) Sequence of event-triggering intervals

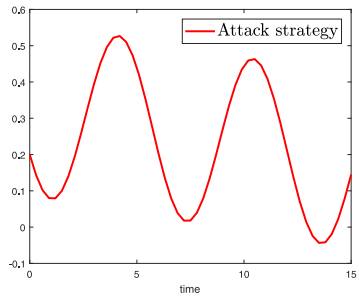

(b) Attack strategy

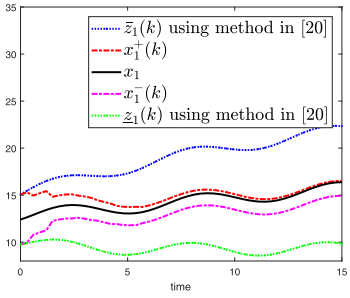

(c) Interval estimation of h_1

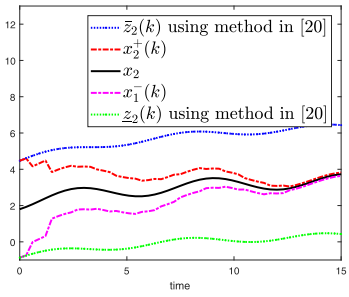

(d) Interval estimation of h_2

Fig. 7. Results of Example 2.

Table 2
The descriptions of the parameters.

Parameter	Description
$h_i^\circ(t)$	The water level of tank i $(i = 1, 2)$
a_i	The cross sectional area of the outlet pipes $(i = 1, 2)$
g	The gravitational acceleration
A_i	The cross section of tank i, $(i = 1, 2)$
γ	The position of the valve
K_p	The pump constant
$\omega(t)$	The disturbances
$v^\circ(t)$	The water flow rate through the pump

parameters are chosen as

$$A = \begin{bmatrix} 0.9842 & 0.0407 \\ 0 & 0.9590 \end{bmatrix}, B = \begin{bmatrix} 0.0007 \\ 0.0352 \end{bmatrix}, J = \begin{bmatrix} 0.08 & 0 \\ 0 & 0.08 \end{bmatrix},$$
$$C = \begin{bmatrix} 0.5 & 0 \end{bmatrix}, D = \begin{bmatrix} 0.5648 \\ 0.1548 \end{bmatrix}, F = -0.4, p_0 = \begin{bmatrix} 12.4 \\ 1.8 \end{bmatrix},$$
$$W = \begin{bmatrix} 1.25 & \\ & 1.25 \end{bmatrix}, \delta = 0.001, \alpha_i = i(i = 1, 2 \ldots, 6),$$
$$u(k) = 3, d(k) = 0.36cos(k) + 0.25, \gamma_1 = 0.2, \gamma_2 = 0.5,$$
$$0 < \gamma = \gamma_2/(1 - \gamma_1) = 0.5/(1 - 0.2) = 0.625 < 1. \tag{82}$$

Similar to Example 1, we take steps to construct the ETIO. By choosing the arbitrary matrix $S = \begin{bmatrix} I_3 & 0 \end{bmatrix} \in R^{3\times 4}$, it is derived from (27) that

$$\begin{bmatrix} \Phi & \Psi \end{bmatrix} = \begin{bmatrix} 1 & 0 & 0 & 0 \\ 0 & 1 & 0 & 0 \\ 1.25 & 0 & 1 & -2.5 \end{bmatrix}. \tag{83}$$

Table 3
Comparison of interval width by the two methods.

	h_1	h_2
The method in [20]	9.5625	5.7789
The proposed method	2.1060	1.5844

By solving LMI (45)–(47), we have a feasible solution

$$P = 142.8262 \times I_6, \eta = 8.6677,$$
$$Q = \begin{bmatrix} 21.0740 & -67.8403 & -0.4601 \\ -67.8403 & 253.8114 & -0.0413 \\ -0.4601 & -0.0413 & 0.5419 \end{bmatrix}, \tag{84}$$
$$L_2 = \begin{bmatrix} -0.3234 & -0.0891 & -0.3963 \end{bmatrix}^T.$$

Following the determination of the gain matrix L_2, the ISS robust observer is constructed and the error dynamics is analyzed by using the SM method. Finally, the interval estimation is accomplished with the simulation results shown in Figs. 7(c)–7(d).

Similar to Example 1, Table 3 is provided to quantitatively illustrate estimation accuracy of the two methods. It can be seen from Figs. 7(c)–7(d) and Table 3 that the estimated intervals produced by the proposed method is of smaller width than that produced by the method in [20]. The simulation results are strong evidences which verify the effectiveness of the proposed method.

5. Conclusion

This paper investigates event-triggered secure estimation for CPSs with UIs. The UIs are treated as augmented state vector, and the resulting descriptor system is derived by introducing a matrix equation as a precondition. To alleviate communication congestion, event-triggered mechanism is considered here and the ETIOs are designed. Based on the assumptions regarding the attack

strategy, its upper and lower bounds are obtained and integrated into the designed ETIO. The interval estimation is accomplished by SE, which is of looser design constraints and more satisfactory accuracy. Examples indicate that compared with the MS method, the proposed method is able to approximately enhance the accuracy of estimation by 4.47 times in Example 1 and 4.54 times in Example 2. Moreover, the interval estimation conducted by the proposed method usually converges within 7.12 s in Example 1 and 5.81 s in Example 2, faster than that by the MS method.

Declaration of competing interest

The authors declare that they have no known competing financial interests or personal relationships that could have appeared to influence the work reported in this paper.

Acknowledgments

The authors are grateful for the support of Natural Science Foundation of Jiangsu Province of China (BK2021-1309) and the Open Fund for Jiangsu Key Laboratory of Advanced Manufacturing Technology, China (HGAMTL-2101).

References

[1] Huang J, Ma X, Che H, Han Z. Further result on interval observer design for discrete-time switched systems and application to circuit systems. IEEE Trans Circuits Syst II Express Briefs 2020;67(11):2542–6.
[2] Efimov D, Raïssi T, Chebotarev S, Zolghadri A. Interval state observer for nonlinear time varying systems. Automatica 2013;49(1):200–5.
[3] Zhang M, Huang J, Zhang Y. Stochastic stability and stabilization for stochastic differential semi-Markov jump systems with incremental quadratic constraints. Internat J Robust Nonlinear Control 2021;31(14):6788–809.
[4] Zheng G, Bejarano FJ, Perruquetti W, Richard J-P. Unknown input observer for linear time-delay systems. Automatica 2015;61:35–43.
[5] Li J, Wang Z, Zhang W, Raïssi T, Shen Y. Interval observer design for continuous-time linear parameter-varying systems. Systems Control Lett 2019;134:104541.
[6] Raïssi T, Videau G, Zolghadri A. Interval observer design for consistency checks of nonlinear continuous-time systems. Automatica 2010;46(3):518–27.
[7] Xie J, Zhu S, Zhang D. Distributed interval state estimation with l_∞-gain optimization for cyber-physical systems subject to bounded disturbance and random stealthy attacks. ISA Trans 2022.
[8] Huong DC, Huynh VT, Trinh H. Interval functional observers design for time-delay systems under stealthy attacks. IEEE Trans Circuits Syst I Regul Pap 2020;67(12):5101–12.
[9] Pan Z, Luan X, Liu F. Confidence set-membership state estimation for LPV systems with inexact scheduling variables. ISA Trans 2022;122:38–48.
[10] Ethabet H, Raïssi T, Amairi M, Combastel C, Aoun M. Interval observer design for continuous-time switched systems under known switching and unknown inputs. Internat J Control 2020;93(5):1088–101.
[11] Wang Y, Gao Y, Wu D, Niu B. Interval observer-based event-triggered control for switched linear systems. J Franklin Inst 2020;357(10):5753–72.
[12] Wang X, Wang X, Su H, Lam J. Coordination control for uncertain networked systems using interval observers. IEEE Trans Syst Man Cybern 2020;50(9):4008–19.
[13] Tang Z, Kuijper M, Chong MS, Mareels I, Leckie C. Linear system security-detection and correction of adversarial sensor attacks in the noise-free case. Automatica 2019;101:53–9.
[14] Li L, Wang W, Ma Q, Pan K, Liu X, Lin L, et al. Cyber attack estimation and detection for cyber-physical power systems. Appl Math Comput 2021;400:126056.
[15] Hu S, Yang F, Gorbachev S, Yue D, Kuzin V, Deng C. Resilient control design for networked DC microgrids under time-constrained DoS attacks. ISA Trans 2022.
[16] Qi Y, Yu W, Zhao X, Xu X. Event-triggered control for network-based switched systems with switching signals subject to dual-terminal DoS attacks. IEEE/ACM Trans Netw 2022;1–11.
[17] He C, Wang J, Liu S, Li J. Fault tolerant control for strict-feedback nonlinear system via event-triggered adaptive algorithms. ISA Trans 2022;126:65–79.
[18] Qu H, Zhao J. Event-triggered H_∞ filtering for discrete-time switched systems under denial-of-service. IEEE Trans Circuits Syst I Regul Pap 2021;68(6):2604–15.
[19] Du S, Liu T, Ho DWC. Dynamic event-triggered control for leader-following consensus of multiagent systems. IEEE Trans Syst Man Cybern 2020;50(9):3243–51.
[20] Li X, Wei G, Ding D. Interval observer design under stealthy attacks and improved event-triggered protocols. IEEE Trans Signal Inf Process Netw 2020;6:570–9.
[21] Degue KH, Efimov D, Le Ny J, Feron E. Interval observers for secure estimation in cyber-physical systems. In: 2018 IEEE conference on decision and control. 2018, p. 4559–64.
[22] Chen Y, Kar S, Moura JMF. Optimal attack strategies subject to detection constraints against cyber-physical systems. IEEE Trans Control Netw Syst 2018;5(3):1157–68.
[23] Zhang H, Cheng P, Shi L, Chen J. Optimal denial-of-service attack scheduling with energy constraint. IEEE Trans Automat Control 2015;60(11):3023–8.
[24] Zhang H, Cheng P, Shi L. Optimal DoS attack scheduling in wireless networked control system. IEEE Trans Control Syst Technol 2016;24(3):843–52.
[25] Zhang J, Zhao X, Zhu F, Karimi HR. Reduced-order observer design for switched descriptor systems with unknown inputs. IEEE Trans Automat Control 2020;65(1):287–94.
[26] Wang Z, Rodrigues M, Theilliol D, Shen Y. Actuator fault estimation observer design for discrete-time linear parameter-varying descriptor systems. Internat J Adapt Control Signal Process 2015;29(2):242–58.
[27] Ethabet H, Rabehi D, Efimov D, Raïssi T. Interval estimation for continuous-time switched linear systems. Automatica 2018;90(90):230–8.
[28] Sontag ED. Input to state stability: Basic concepts and results. Lecture Notes in Math 2008;163–220.
[29] Jiang B, Wang JL, Soh YC. An adaptive technique for robust diagnosis of faults with independent effects on system outputs. Internat J Control 2002;75(11):792–802.
[30] Mazenc F, Bernard O. Interval observers for linear time-invariant systems with disturbances. Automatica 2011;47(1):140–7.
[31] Raïssi T, Efimov D, Zolghadri A. Interval state estimation for a class of nonlinear systems. IEEE Trans Automat Control 2012;57(1):260–5.
[32] Tang W, Wang Z, Wang Y, Raïssi T, Shen Y. Interval estimation methods for discrete-time linear time-invariant systems. IEEE Trans Automat Control 2019;64(11):4717–24.
[33] Pourasghar M, Puig V, Ocampo-Martinez C. Interval observer versus set-membership approaches for fault detection in uncertain systems using zonotopes. Internat J Robust Nonlinear Control 2019;29(10):2819–43.